International Journal of Information technology and Computer Engineering
ISSN: 2455-5290
Vol: 04, No. 06, Oct-Nov 2024
http://journal.hmjournals.com/index.php/IJITC
DOI: https://doi.org/10.55529/ijitc.46.1.17

Design of an Objective Magnetic Lens and Study of its Magnetic and Optical Properties in the Scanning Electron Microscope

Nabaa Burhan Ali Mohammed[1*], Mohammed Abdullah Hussein[2]

[1] Master student, Department of Physics,College of Sciences,University of Kirkuk, Kirkuk, Iraq.*
[2] Assistant Professor, Department of physics, College of Education for Girls, University of Kirkuk, Kirkuk, Iraq.

Email: [2]mohdphy@uokirkuk.edu.iq
Corresponding Email: [1]scpm23007@uokirkuk.edu.iq*

Received: 02 June 2024 **Accepted:** 16 August 2024 **Published:** 01 October 2024

Abstract: ***The study's objective is to investigate the optical properties of the objective magnetic lens, which is considered as the most crucial part of the electron microscope. Three models of objective lenses (Snorkel, Pinhole, Gemini), equal in geometric dimensions were taken, and their optical properties, as well as their magnetic properties. It was found that the lens (P) achieved the best results, which were studied at a continuous excitation (NI=2000 A-t) and different acceleration voltages ranging from (8-16 kV), in addition to different values for the aperture angle (α). Then, we conducted an improvement on the selected lens by changing the width of the air gap between the poles (S) and studying the properties of the lens. We obtained better results for spherical (Cs=1.62 mm) and chromatic (C_c=1.84 mm) aberrations, focal length (f_o=2.92 mm), as well as the highest value of the magnetic field (B_z=0.38 T) at an acceleration voltage (V_r=10000 V), excitation (NI=2000 A-t), and air gap width (S=5 mm), and the diameter of the electron probe (dp=11.25 nm) at an aperture angle (α=2 mrad).***

Keywords: Objective Lens, Scanning Electron Microscope, Optical Properties for Objective Lens, Magnetic Properties.

1. INTRODUCTION

In 1926, the concept of the general theory for the motion of electrons and ions was introduced by the scientist Hans Busch, who laid the theoretical foundations for the movement of charged particles based on De Broglie's hypothesis. Busch demonstrated that the magnetic field's impact on a charged beam resembles to that of a glass lens on a visible light beam

International Journal of Information technology and Computer Engineering
ISSN: 2455-5290
Vol: 04, No. 06, Oct-Nov 2024
http://journal.hmjournals.com/index.php/IJITC
DOI: https://doi.org/10.55529/ijitc.46.1.17

passing through it [1]. Busch investigated the motions of charged particles in magnetic and electric fields that are axially symmetric. The foundations of electron optics were laid when he proved that these fields could function as objective lenses [2]. Electron optics can be defined as the branch that deals with the movement of charged particles and their focusing using electric or magnetic fields, and the formation of precise images of the sample surface. The electron beam used in electron optics is very narrow, allowing its cross-sectional area to be negligible [3]. This series of discoveries led to a rapid development in the field of electron optics, this therefore prompted scientists Knoll and Ruska to create the first electron microscope in 1931, with an acceleration voltage of (50 kV) and a magnification of (16) times [4]. The electron microscope can be defined as a device that is used to Focusing a beam of electrons and project it onto a specimen to obtain a clear image [5]. The transmission electron microscope and the scanning electron microscope are the two primary varieties of electron microscopes. The transmission electron microscope is a tool that creates two-dimensional pictures of a very thin sample by passing a high-voltage electron beam across it. These images reveal details about the internal structure of the sample. The transmission microscope has a high magnification power that can reach up to 2 million times. In cases that require high precision in imaging, the thickness of the sample is very thin, less than (30 nm) [6]. The transmission electron microscope consists of three main parts: (Illuminating System - Imaging System - Recording System). The scanning electron microscope: is a device that operates by accelerating a narrow beam of electrons in the electron gun to high speeds and then passing it through magnetic lenses, which leads to their convergence and magnification so that they focus on the surface of the sample. After the dispersed electrons leave the sample's surface, the detector gathers them and transforms them into a signal amplifier, which amplifies the signal and sends it to the screen to create a three-dimensional image of the sample's surface [2]. Compared to a transmission microscope, the scanning electron microscope provides higher accuracy and lower magnification for examining the outside surface of relatively thick and large materials. The analytical capability of this microscope depends on the diameter of the electron probe focused on a very small area, ranging in diameter from about (5-10 nm) [6]. The scanning electron microscope consists of three main parts: (Illuminating System - Electron Gun - Imaging System). The sorts of objective lenses that make up the scanning electron microscope's lighting system will be the subject of this research project. The main purpose of this lens, which focuses the electron beam descending on the sample to create a picture of it, is why it is termed an objective lens. It is the electron microscope's most crucial component. It is crucial that this lens has a high resolving power since it affects the electron microscope's capacity to resolve images [7]. This lens also contributes to spherical and chromatic aberrations more than other lenses, which is why it is important to take into account the precision of the design and manufacturing of this lens. [8]. There are three types of objective lenses according to the location of the eyepiece in the scanning electron microscope: Pinhole Lens: The sample’s location and its magnetic field are outside the lens, and the model is defined by the size of the sample chamber, not the size of the lens. Therefore, it is suitable for use with large models. This lens has large focal lengths ranging from (5-40 nm) and can be used to produce images with high depth of field because the working distance within it is variable. However, this lens is not used in high-resolution analyses because it has high aberration values. One of the disadvantages of this lens is that its

International Journal of Information technology and Computer Engineering
ISSN: 2455-5290
Vol: 04, No. 06, Oct-Nov 2024
http://journal.hmjournals.com/index.php/IJITC
DOI: https://doi.org/10.55529/ijitc.46.1.17

performance is classified as weak at low voltages [9] [10]. Snorkel Lens: The sample is situated outside the lens yet inside within its magnetic field, as the magnetic field extends outward to reach the sample [11]. This lens may be used with big samples since the lens gap does not restrict the size of the sample. The low aberration coefficients of this lens are one of its benefits [12]. Gemini Lens: This lens combines electric and magnetic fields, possesses an electron beam enhancement system, and also has an annular detector inside the lens that serves to reduce field effects and improve the clarity of the sample image [13].

2. RELATED WORKS

[14] Developed a physical magnetic lens and analyzed its optical properties using simulation programs based on the finite element method. They designed a magnetic lens with asymmetric dual poles and concluded from the research that the distance between the poles has a clear impact on the optical properties of the magnetic lens. The study found that as the distance decreases, the spherical aberration C_s, chromatic aberration C_c, focal length f_o, and electron probe diameter dp improve. Additionally, the aperture angle α in the lens plays a significant role in determining the resolution δ by setting the minimum electron probe diameter to achieve minimal aberration. [13] examined how the length of the outer pole affected the focal length (f_o), spherical aberration (Cs), chromatic aberration (Cc), axial magnetic field distribution (Bz), and electron probe diameter (dp) of a Gemini lens in order to improve optical qualities. The researcher came to the conclusion that the optical and focusing characteristics of the physical lenses are significantly affected by altering the length of the outer pole on the side of the magnetic lens. [15] Utilized the Finite Element Method for Magnetic Field Calculation (FEM-CMFD) and the Magnetic Electron Lens Optical Properties Evaluation (MELOPE) program to evaluate three novel designs for the pinhole magnetic lens and investigate their optical and magnetic characteristics. [10] Designed a magnetic lens using analytical optimization and the Finite Element Method, with assistance from the Munro software. Using the Electron Optical Design (EOD) application, the researcher was able to shed light on how the air gap S functionsed in the magnetic lens's design. According to the study's findings, changes in the air gap have a major effect on how well magnetic lenses work, with smaller air gaps producing noticeably better optical and focal length results. On the other hand, when the air gap is increased, the maximum magnetic field value decreases and the axial magnetic field half-width increases. This emphasizes how crucial it is to precisely optimize the air gap in order to get the required lens performance. [16] Designed four identical geometrically sized versions of the Gemini-type magnetic pinhole lens with the same coil size. They swiftly obtained optical property findings for the suggested models by utilizing state-of-the-art algorithms. The focus length, electron probe diameter, and spherical and chromatic aberration coefficients were found to be significantly affected by variations in the distance between the poles. They came to the conclusion that in order to create a lens with superior optical qualities, lowering the distance between the poles lowers the focal length, electron probe diameter, aberration coefficients, and analysis capabilities.

International Journal of Information technology and Computer Engineering
ISSN: 2455-5290
Vol: 04, No. 06, Oct-Nov 2024
http://journal.hmjournals.com/index.php/IJITC
DOI: https://doi.org/10.55529/ijitc.46.1.17

3. METHODOLOGY

The Programs Used in this Study

The Finite Element Method (FEM)

In 1945, the scientist Courant proposed the method of finite elements, which is one of the most important methods used in the fields of engineering and physics, requiring solving complex differential equations. In 1973, this method was used in the field of electron optics by the scientist Munro, who was the first to use it in this field to calculate the magnetic fields of round magnetic lenses. In this method, the lens and its surrounding area are accurately divided into specific elements using axial lines and radial lines, creating a coarse mesh due to the intersection of axial lines with radial lines. These meshes are then further divided into finer secondary divisions called fine meshes, with denser lines concentrated at the coil, lens diameter, air gap, and poles. The density gradually decreases as we move closer to the outer boundaries of the lens structure, as shown in Figure 1, illustrating the distribution of coarse and fine lines on the lens [17]. This method is characterized by its ease in handling any pole shape, calculating magnetic flux density distribution, precise analysis of magnetic circuits, and is also used in calculating the electric and magnetic fields of electron lens.

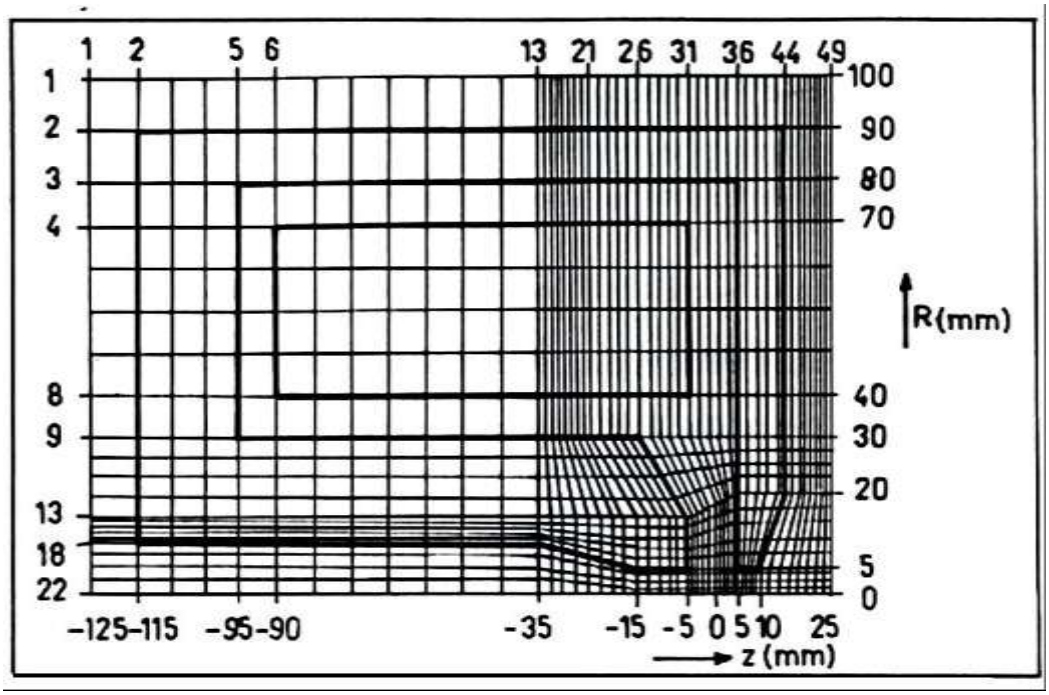

Fig. 1 shows the distribution of coarse and fine mesh lines on the upper dimensions of the magnetic lens.

Program (AMAG)

The AMAG program is one of the important programs, developed by the scientist Lencovà in 1986, and it operates based on the Finite Element Method (FEM). This program is characterized by its high accuracy due to its ability to accommodate a large number of mesh

International Journal of Information technology and Computer Engineering
ISSN: 2455-5290
Vol: 04, No. 06, Oct-Nov 2024
http://journal.hmjournals.com/index.php/IJITC
DOI: https://doi.org/10.55529/ijitc.46.1.17

lines similar to those used in the Munro program. The program computes the voltage vector for every rotationally symmetric magnetic lens in addition to the value of the axial magnetic flux density of the lens. In addition, it computes the magnetic flux density in the magnetic circuit and uses the axial magnetic flux density distribution to calculate the lens excitation.
Furthermore, it addresses the magnetic saturation phenomenon and calculates the magnetic flux density in saturated lenses. The AMAG program can handle various magnetic circuits made of one or more materials with different magnetization curves (B-H curves), such as soft iron and permendur. Additionally, this program can handle up to ten different excitations [18].

Program (M21)
The axial magnetic flux for magnetic lenses is first computed using the AMAG program, and then the optical parameters of the lenses are determined using this program, which was created by scientist Munro in 1975. For a given range of operating voltages (V_r), this software can handle zero, low, high, or infinite magnification circumstances. The object plane (Z_o), image plane (Z_i), effective focal length (f_o), excitation factor ($NI/V_r1/2$), chromatic aberration coefficient (Cc), spherical aberration coefficient (Cs), and magnetic flux density at the object or image plane level are among the other characteristics that may be computed by the application. Using the Simpson Rule for magnetic lenses, the spherical aberration coefficient (Cs) and chromatic aberration coefficient (Cc) are computed numerically to the object plane Z_o or the image plane Z_i, as indicated in the following equations. (2-2) و (2-4) [19]

The focal length of the magnetic lens can also be calculated from the following equation:

$$\frac{1}{f_m}=\int_{Z_o}^{Z_i}\frac{e}{8mV_r}B_z^2dz \qquad (3\text{-}1)$$

Where V_r represents the relatively corrected voltage.

Paraxial Trajectory of Electrons Computation of the Magnetic Lens
Using the program (M21), the parallel electron path to the axis R (z) is calculated, and the program uses the fourth-order Runge - Kutte method to solve the axial ray equation. [20].

The axial ray equation is represented by the following relationship [3]:

$$R''(z)+\frac{e}{8mV_r}B_z^2R(z)=0 \qquad (3\text{-}2)$$

Where R" (z) is the second derivative of the electron beam height.

B_z is the magnetic flux density of the lens.

$$R(z+h)=R(z)R'(z)h+(k_1+k_2+k_3)h/6 \qquad (3\text{-}3)$$

$$R'(z+h)=R'(z)+(k_1+2k_2+2k_3+k_4)/6 \qquad (3\text{-}4)$$

Where:

International Journal of Information technology and Computer Engineering
ISSN: 2455-5290
Vol: 04, No. 06, Oct-Nov 2024
http://journal.hmjournals.com/index.php/IJITC
DOI: https://doi.org/10.55529/ijitc.46.1.17

$k_1 = h\ f(z)\ \ R(z)\ ;\ f(z) = \frac{-e}{8mV_r} B_z^2$

$k_2 = h\ f(z + h/2\ )(R(z) + h\ \ R^{'}(z)/2\ )$

$k_3 = h\ f(z + h/2\ )(R(z) + h\ R^{'}/2 + k_1\ h/4$

$k_4 = h\ f(z+h)(R(z) + h\ R^{'}(z) + k_2\ h/2$

And R'(z) represents the first derivative of R (z), (k_1, k_2, k_3, k_4) represent the Runge-Kutta coefficients, h is the increment value each time.

Program Flux (M31)

In 1975, the scientist Munro developed the program, is used to draw the trajectories of magnetic flux lines for magnetic lenses. It was named Flux and was modified by the researcher Murad in 1998. This program is supplied with the magnetic flux values obtained from the AMAG program. Then, the magnetic flux values are calculated at each point of the finite element meshes and stored in a specific file to be input into the Flux program. To draw the magnetic flux lines the program connects the magnetic flux points at each point of the mesh points that have the same voltage values. These lines concentrate around the iron poles of the lens, taking circular shapes and being sparse in low-density areas and convergent in high-density areas [21].

Electron Optical Design Program (EOD)

The EOD program is an advanced tool for designing optical systems for charged particles. It was first presented in the year 2000 during the EUREM conference in Bano. The program has received wide acclaim at numerous conferences in Europe, described as the most comprehensive. After years of development, the program has reached a mature stage [22]. Users of the program may compute fields with rotational symmetry magnetic and electrostatic lenses, as well as for multi-pole lenses using the finite element method. The program also helps in tracking the paths of charged particles by calculating electric and magnetic fields, allowing for graphical representations and particle properties along the ray axis or at specific planes. The program calculates the chromatic and spherical aberration coefficients for optical systems. Figure 2 shows the grid used in designing symmetrical magnetic lenses, consisting of horizontal and vertical lines used in the EOD program. The input grid lines are defined as rough quadrilateral lines, with resulting subdivisions shown as smoothly graded lines in the same figure. Appropriate voltage function values are calculated at the nodes according to the finite element method within the EOD program. Furthermore, the program displays results and evaluates the optical and magnetic properties of the lens based on magnetic field calculations and tracking the path of the electron beam passing through it [23]

International Journal of Information technology and Computer Engineering
ISSN: 2455-5290
Vol: 04, No. 06, Oct-Nov 2024
http://journal.hmjournals.com/index.php/IJITC
DOI: https://doi.org/10.55529/ijitc.46.1.17

Fig. 2 the grid lines used in the calculations for designing symmetrical magnetic lenses [23].

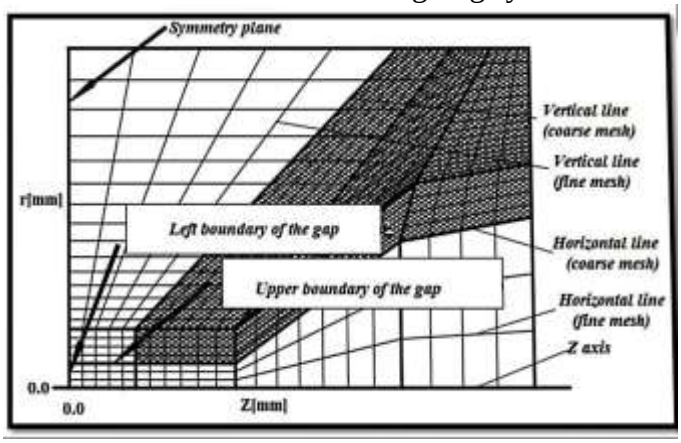

4. RESULTS AND DISCUSSIONS

Three models of objective lenses were taken (Snorkel, Pinhole, Gemini), denoted by the symbols (S, P, G) respectively, were obtained. These lenses have equal dimensions, as shown in Fig. 3. The study focused on their optical properties, including chromatic aberration (C_c), spherical aberration (C_s), focal length (f_o), and the diameter of the electron probe (dp). Additionally, their magnetic properties were investigated, specifically of the magnetic field intensity (B_z).

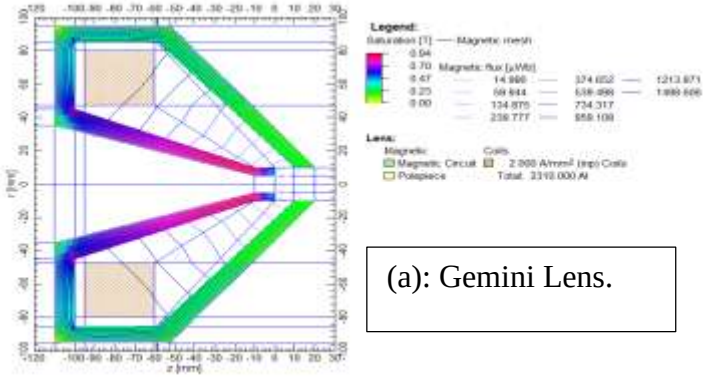

(a): Gemini Lens.

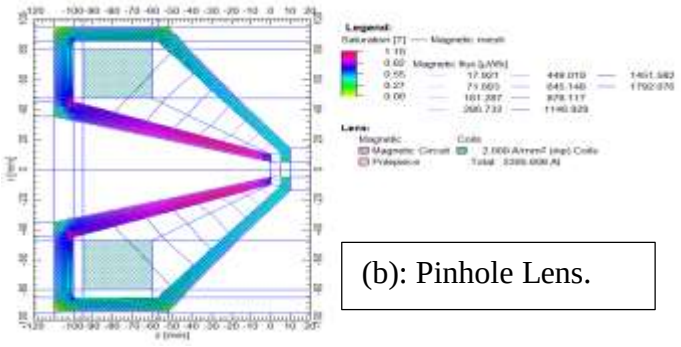

(b): Pinhole Lens.

International Journal of Information technology and Computer Engineering
ISSN: 2455-5290
Vol: 04, No. 06, Oct-Nov 2024
http://journal.hmjournals.com/index.php/IJITC
DOI: https://doi.org/10.55529/ijitc.46.1.17

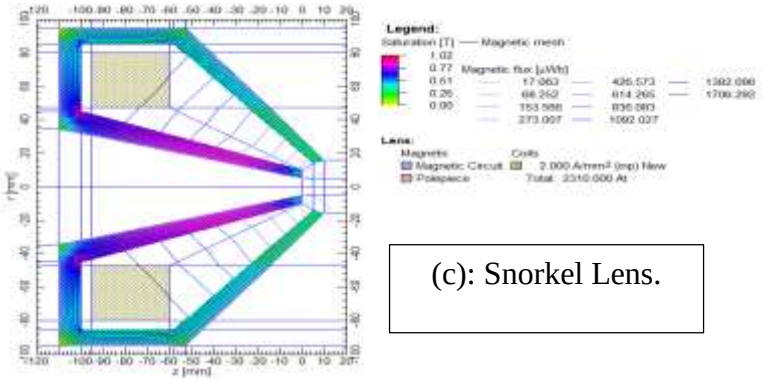

(c): Snorkel Lens.

Fig.3. 2D drawing of three lenses (Snorkel, Pinhole, Gemini).

The figures 4, 5, and 6, illustrate the chromatic aberration (C_c), spherical aberration (C_s), and focal length (f_o), respectively, for the three lenses (S, P, G). At different values of accelerating voltages (V_r) and with a constant excitation for the lens (NI = 2000 A-t). We notice from these shapes that the values of aberration and focal length increase with higher acceleration voltages. Notably, the Pinhole lens (P) have the lowest values for both aberration coefficients and focal length among the three lenses. Consequently, the Pinhole lens achieved the most favorable results.

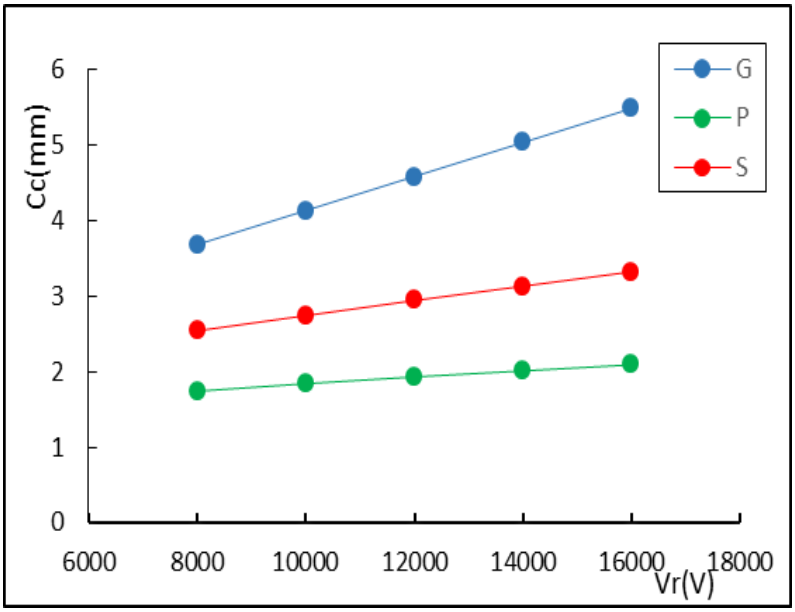

Fig.4. Chromatic aberration (C_c) values for the three lenses at different values of acceleration voltages (V_r) with lens excitation constant (NI=2000 A-t).

International Journal of Information technology and Computer Engineering
ISSN: 2455-5290
Vol: 04, No. 06, Oct-Nov 2024
http://journal.hmjournals.com/index.php/IJITC
DOI: https://doi.org/10.55529/ijitc.46.1.17

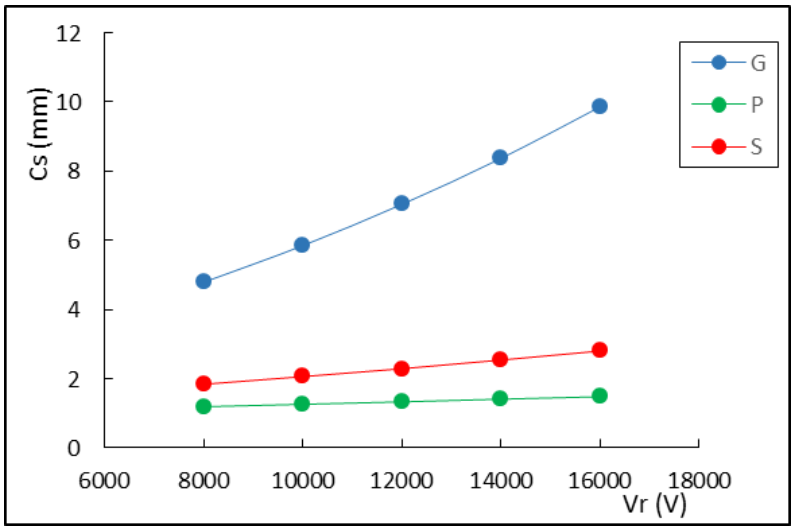

Fig.5. Spherical aberrations (C_s) values for the three lenses at different values of acceleration voltages (V_r) with lens excitation constant (NI=2000A-t).

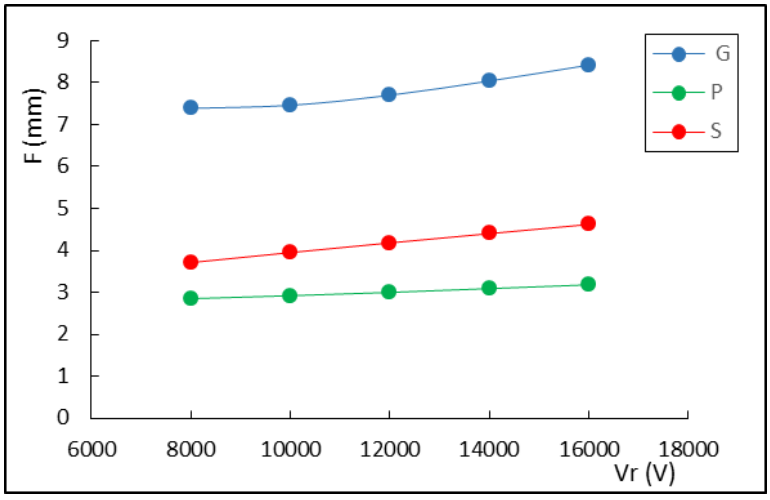

Fig.6. Focal length (f_o) values for the three lenses at different values of acceleration voltages (V_r) with lens excitation constant (NI=2000A-t).

Figure 7 illustrates the values of aberrations for chromatic (ds), spherical (dc), Gaussian (dg), and diffraction (dd), as well as the diameter of the electron probe (dp) for the three lenses (S, P, G), at different values of the aperture angle (α) With constant accelerating voltage (V_r = 10 kV), and constant excitation for lens (NI = 2000 A-t). And we notice from the figure that the aberrations chromatic and spherical (ds, dc) increase with an increase in the aperture angle. Conversely, Gaussian and diffraction aberrations (dg, dd) decrease as the aperture angle increases. As well as that the diameter of the electron probe (dp) initially decreases and then increases again. Therefore, there exists an optimal aperture angle through which we obtain the best result for the aberrations and diameter of the electron probe, which is (α = 2 mrad).

International Journal of Information technology and Computer Engineering
ISSN: 2455-5290
Vol: 04, No. 06, Oct-Nov 2024
http://journal.hmjournals.com/index.php/IJITC
DOI: https://doi.org/10.55529/ijitc.46.1.17

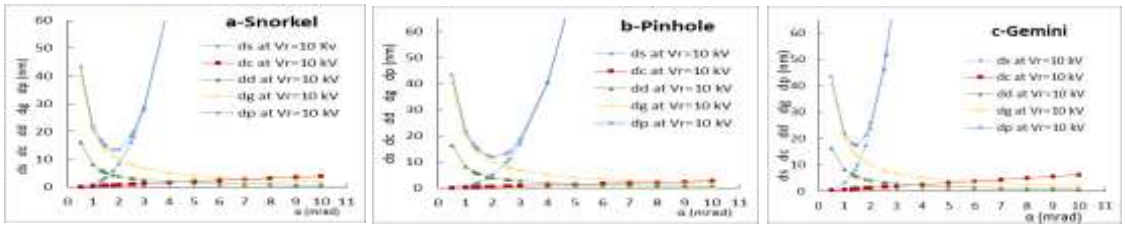

Fig. 7. Values of (dc, ds, dd, dg & dp) for the three lenses at different values of the aperture angle (α) with constant acceleration voltage (V_r=10 kV) and with lens excitation constant (NI=2000 A-t).

Figure 8 illustrates the values of the electron drope diameter (dp) for the three lenses at different aperture angles (α), with a constant acceleration voltage (V_r = 10 kV) and with lens excitation constant (NI = 2000 A-t). We notice that the (dp) values for the three lenses initially decrease at a certain aperture angle and then it increases again with increasing aperture angle. The Pinhole lens (P) achieved the best value for the electron probe diameter (dp=11.25 nm), at an aperture angle of (α=2 mrad).

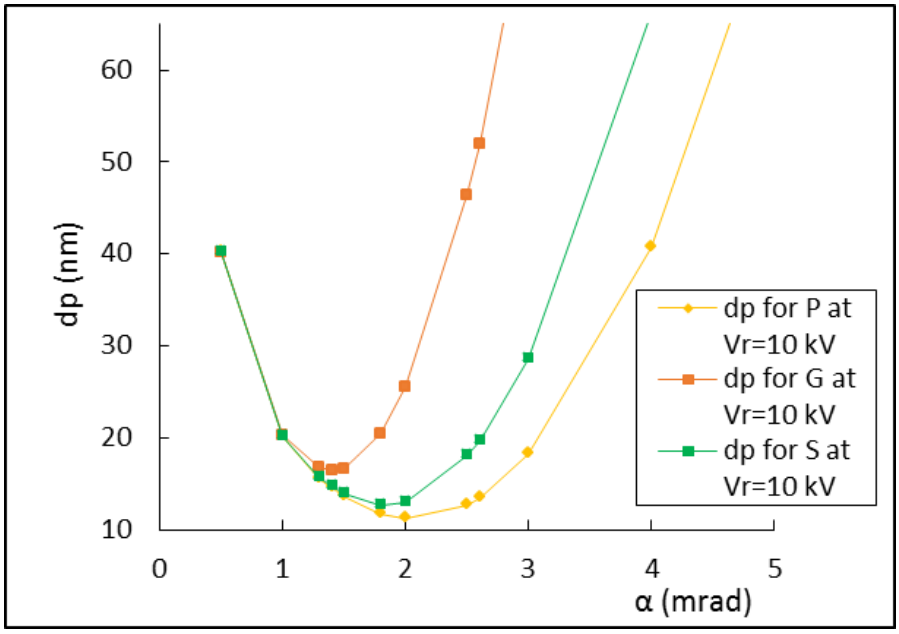

Fig.8. Electron probe diameter (dp) values for the three lenses at different values of the aperture angle α) with a fixed value of the acceleration voltage (V_r=10 kV) and with lens excitation constant (NI=2000 A-t).

Figure 9 illustrates the resolving power (δ) values for the three lenses (S, P, G) at different accelerating voltages (V_r). It can be observed from the figure that the values of (δ) decrease with an increase in the accelerating voltage. It was noted that lens (P) possesses the lowest resolving power with less aberration compared to lenses (S) and (G), where the resolving power helps to determine the effectiveness of the lens.

International Journal of Information technology and Computer Engineering
ISSN: 2455-5290
Vol: 04, No. 06, Oct-Nov 2024
http://journal.hmjournals.com/index.php/IJITC
DOI: https://doi.org/10.55529/ijitc.46.1.17

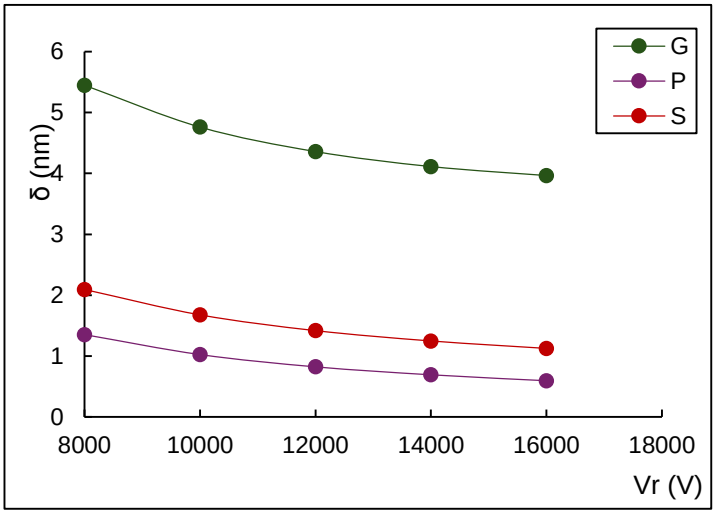

Fig.9. Values of resolving power (δ) of the three lenses (S, P, G) at different values of acceleration voltages (V_r).

Figure 10. Demonstrates the magnetic properties that were studied for the three lenses, represented by the magnetic field intensity (B_z) as a function of the optical axis (Z) at a constant excitation (NI=2000 A-t). It is observed that the magnetic flux near the pole region has a maximum value (B_{max}), and it was found that lens (P) has the highest value of (B_{max}) among the three lenses, indicating that lens (P) possesses good focusing properties.

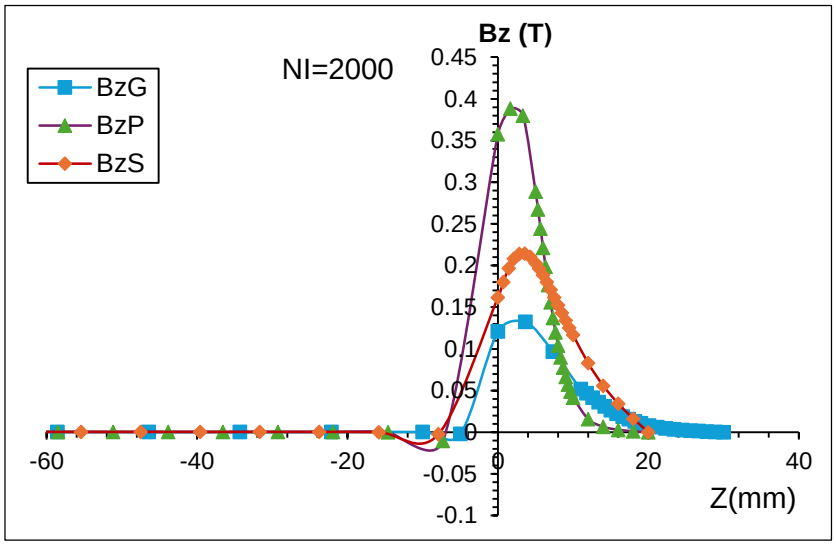

Fig.10. Distribution of magnetic field strength (B_z) for the three lenses as a function of the optical axis (Z) at constant excitation (NI=2000 A-t).

After selecting the best model from the three lenses, which was represented by lens (P), we conducted an optimization on this lens by changing the width of the air gap between the poles by taking different values as follows (S=5,8,11,14,17)mm. These were referred to by the

International Journal of Information technology and Computer Engineering
ISSN: 2455-5290
Vol: 04, No. 06, Oct-Nov 2024
http://journal.hmjournals.com/index.php/IJITC
DOI: https://doi.org/10.55529/ijitc.46.1.17

following symbols (P_1,P_2,P_3,P_4,P_5) respectively, as shown in Figure 11. Their optical and magnetic properties were studied at different accelerating voltage values ranging from (8000-16000) V and at a constant excitation (NI=2000 A-t).

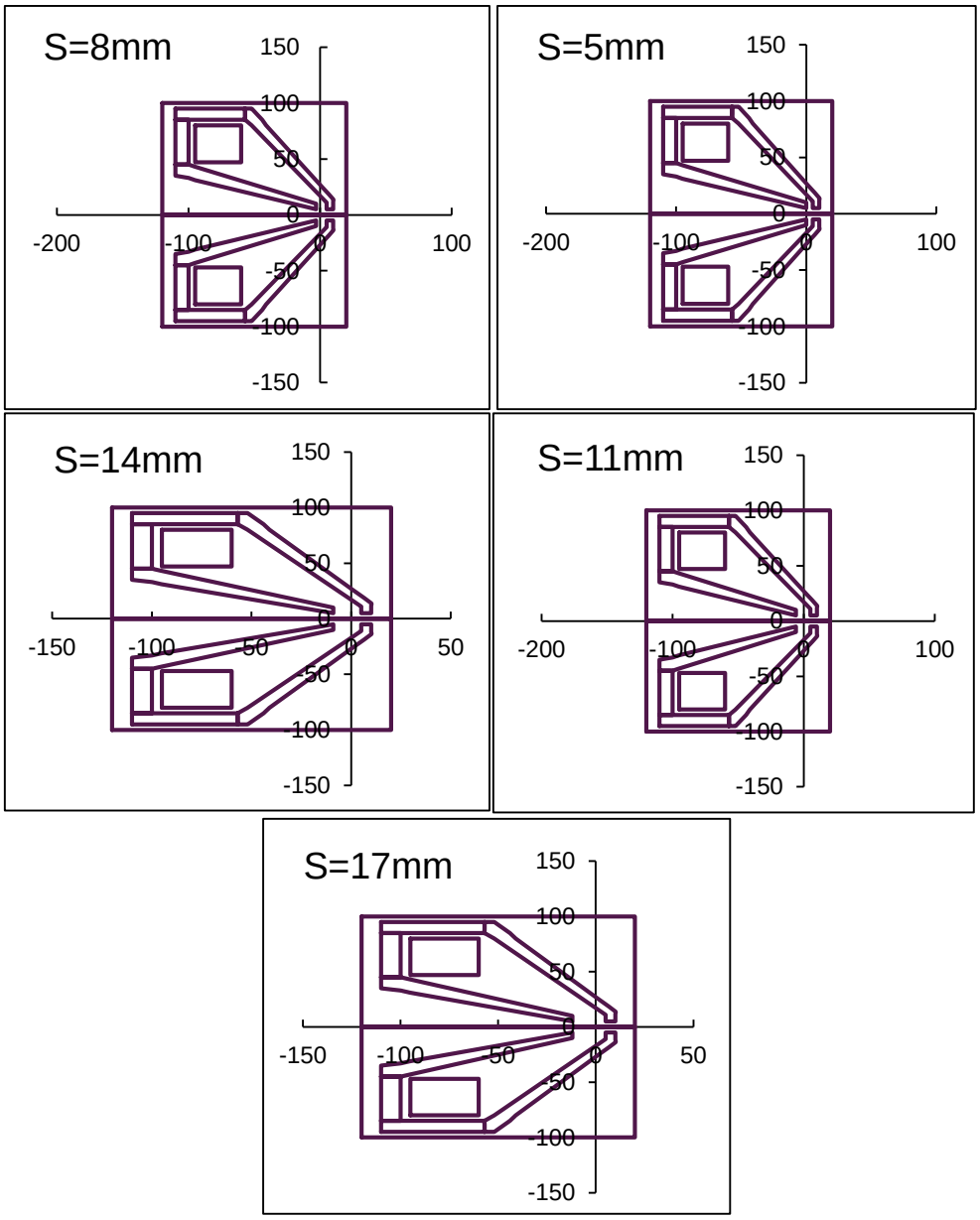

Fig.11. Models of pinhole lens when changing the width of the air gap between the Poles (S).

Figures 12, 13, and 14 , illustrate the values of chromatic aberration (C_c), spherical aberration (C_s), and focal length (f_o) respectively for the lens models (P_1, P_2, P_3, P_4, P_5), which had their air gap width altered at different accelerating voltage (V_r) values while maintaining a constant lens excitation (NI=2000 A-t). These figures show that the aberration values and focal length are directly proportional to the accelerating voltage; the lower the accelerating

International Journal of Information technology and Computer Engineering
ISSN: 2455-5290
Vol: 04, No. 06, Oct-Nov 2024
http://journal.hmjournals.com/index.php/IJITC
DOI: https://doi.org/10.55529/ijitc.46.1.17

voltage, the better the aberration values and focal length obtained. It is observed that the model P1 (S=5 mm) has the lowest values of chromatic aberration (C_c), spherical aberration (C_s), and focal length (f_o) among the five models.

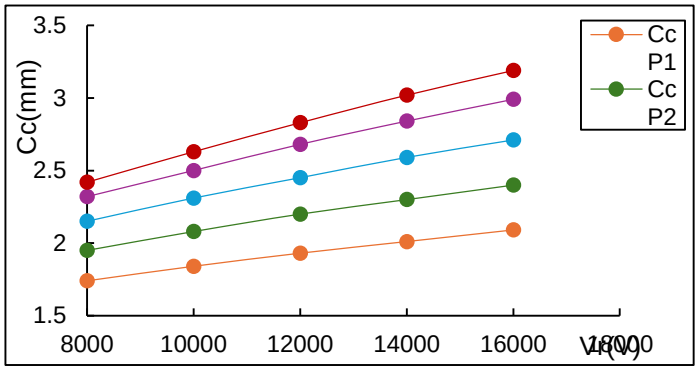

Fig.12. Chromatic aberration (C_c) values of models for lens (P) at different values of acceleration voltages (Vr) with lens excitation constant (NI=2000 A-t).

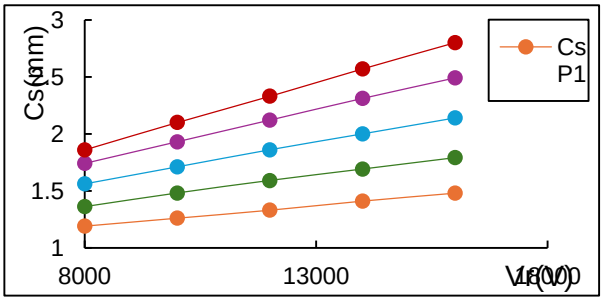

Fig.13. Spherical aberration (Cs) values of models for lens (P) at different values of acceleration voltages (Vr) with lens excitation constant (NI=2000 A-t).

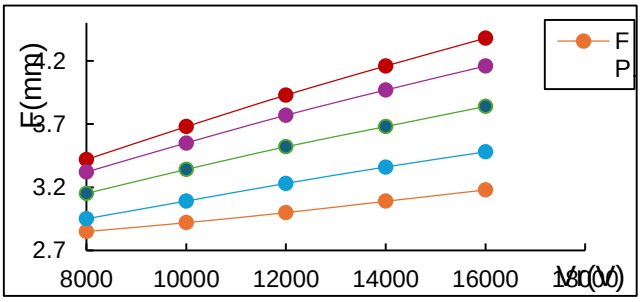

Fig.14. Focal length (f_o) values of models for lens (P) at different values of acceleration voltages (Vr) at constant excitation (NI=2000 A-t).

Figure 15 illustrates the values of chromatic aberration (C_c), spherical aberration (Cs), and focal length (f_o) for the five models as a function of the air gap width (S) at a constant acceleration voltage (V_r=10 kV) and constant excitation (NI=2000 A-t). The figure shows that the values of aberrations (C_c), (C_s) and focal length (f_o) increase as the air gap width (S) increases, leading to poor optical properties, as indicated in Table. This is due to the increase

International Journal of Information technology and Computer Engineering
ISSN: 2455-5290
Vol: 04, No. 06, Oct-Nov 2024
http://journal.hmjournals.com/index.php/IJITC
DOI: https://doi.org/10.55529/ijitc.46.1.17

in the width of the axial magnetic field's half-width (W). Therefore, it is observed that the lens (P1) with an air gap width (S=5 mm) possesses better optical properties among the five lenses because it has lower values of aberrations and focal length.

Table 1 shows the change in optical properties with the width of the air gap (S) with constant acceleration voltage (V_r=10 kV) and constant excitation (NI=2000 A-t).

S (mm)	C_c (mm)	C_s (mm)	f_o (mm)
5	1.84	1.26	2.92
8	2.08	1.48	3.09
11	2.31	1.71	3.34
14	2.5	1.93	3.55
17	2.63	2.1	3.68

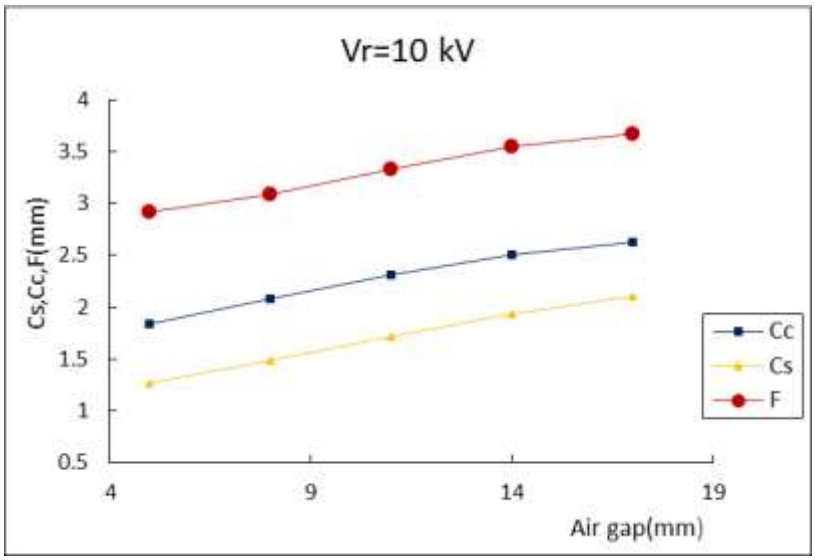

Fig.15. Curves of chromatic (C_c), spherical (C_s) and focal length (f_o) aberrations for the five models at different values of air gap width (S) with constant acceleration voltage (V_r=10 kV) and constant excitation (NI=2000 A-t).

Figure 16. shows the magnetic field strength (B_z) of the five models for different values of air gap width at constant excitation (NI = 2000 A-t). It can be seen from the figure that the maximum value of the magnetic field intensity (B_{max}) decreases with increasing air gap width and vice versa. The highest value of the magnetic field intensity of the lens (P1) was obtained at (B_z=0.38T).

International Journal of Information technology and Computer Engineering
ISSN: 2455-5290
Vol: 04, No. 06, Oct-Nov 2024
http://journal.hmjournals.com/index.php/IJITC
DOI: https://doi.org/10.55529/ijitc.46.1.17

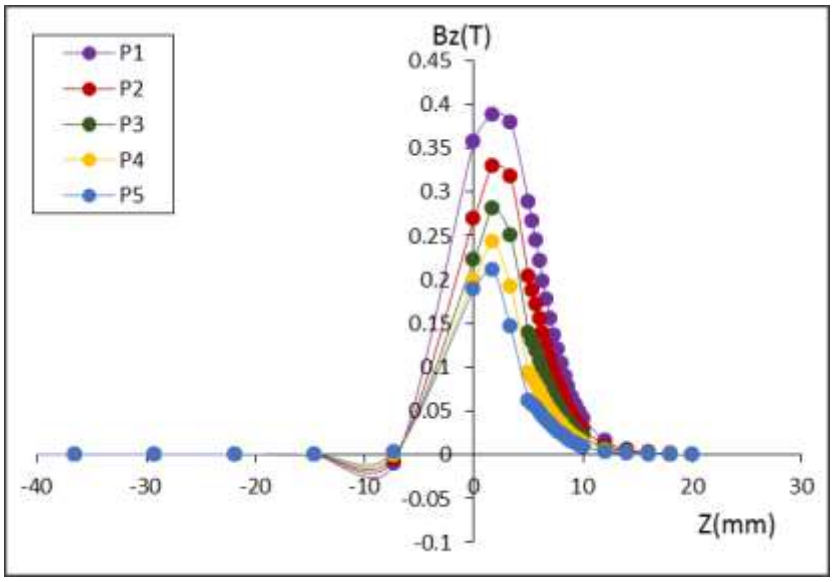

Fig.16. Magnetic field strength (B_z) for different values of air gap width at constant excitation (NI=2000A-t).

5. CONCLUSIONS

After the study, it was concluded that the type of lens directly affects the optical properties, as lens of type (P) were found to have minimal aberrations and a small electron probe diameter. Similarly, regarding the air gap width between the poles, after making improvements to the optimal lens (P) among the three studied lenses (S, P, G) by changing the air gap width, it was shown that the smaller the air gap width, the better the results for aberrations, thus obtaining a lens with good focusing properties. Therefore, the lens with an air gap width (S=5 mm) achieved the best results. It was also concluded that the maximum value of the magnetic field intensity (B_{max}) is inversely proportional to the air gap width; the smaller the air gap width, the greater the magnetic field intensity (B_{max}). Additionally, it was found that the electron probe diameter decreases at certain values of the aperture angle (α) and then begins to increase again, indicating that there is an optimal aperture angle value that yields the best result for the electron probe diameter. Moreover, the Gaussian aberration and diffraction aberration decreases with the aperture angle, while spherical and chromatic aberrations increase with the aperture angle, hence there is a suitable value at which the aberrations and the electron probe diameter are minimized.

6. REFERENCES

1. F. Haguenau, P. W. Hawkes, J. L. Hutchison, B. Satiat-Jeunemaître, G. T. Simon, and D. B. Williams, 'Key events in the history of electron microscopy', Microsc. Microanal., vol. 9, no. 2, p. 96, 2003.
2. H. H. Rose, 'Optics of high-performance electron microscopes', Sci. Technol. Adv. Mater., vol. 9, no. 1, p. 14107, 2008.

International Journal of Information technology and Computer Engineering
ISSN: 2455-5290
Vol: 04, No. 06, Oct-Nov 2024
http://journal.hmjournals.com/index.php/IJITC
DOI: https://doi.org/10.55529/ijitc.46.1.17

3. M. K. A. AL-Janan, and R. Y. J. AL-Salih, "Design and studying the effect of Polepiece shape on the magnetic and optical properties of the unipolar lens", Tikrit Journal of Pure Science Vol. 27 (6) 2022, ISSN: 1813 – 1662, E-ISSN: 2415 – 1726.
4. F. Haguenau, P. W. Hawkes, J. L. Hutchison, J. B. Satiat, G. T. Simon, D. B. Williams, (2003),:Key events in the history of electron microscopy ", Microscopy and Microanalysis, Vol. 9, No. 2, pp.96-138.
5. J. J. Bozzola and L. D. Russell, Electron microscopy: principles and techniques for biologists. Jones & Bartlett Learning, 1999.
6. C. Y. Tang and Z. Yang, "Transmission electron microscopy (TEM)", in Membrane characterization, Elsevier, 2017, pp. 145–159.
7. M. J. Ahmed and M. A. Hussein, "Computation Design to Simulate an Objective Magnetic Lens and Study of Effect the Distance Between Pole pieces on its Optical Properties", Journal of Current Researches on Educational Studies, 12 (2), 67-76, 2022.
8. P. W. Hawkes, "Principles of Electron Optics", Volume 2_ Applied Geometrical Optics. 2-Academic Press, 2017, Ch36.ph771.
9. H. Chen, Q. Dong, H. Wang, and Z. Yang, 'Optical simulation analysis and study of UTEM electron gun', in Journal of Physics: Conference Series, 2021, vol. 2012, no. 1, p. 12044.
10. R. S. Ali, M. A. Hussein and R Y. J. AL-Salih, "Optimizing the Effectiveness of Magnetic Lenses by utilizing the Electron Optical Design (EOD) Software", Engineering, Technology & Applied Science Research, Vol. 13, No. 6, 2023, 11980-11984, 12 September 2023.
11. J. I. Goldstein, D. E. Newbury, J. R. Michael, N. W. Ritchie, J. H. J. Scott, and D. C. Joy, "Scanning electron microscopy and X-ray microanalysis". Springer, 2017.
12. S. M. Juma, and T. Mulvey, "The axial field distribution of single polepiece lenses". In Inst. Phys. Conf. Ser Vol. 52, pp. 59-60, 1980.
13. E. A. Othman and M. A. Hussein, "Effect of Outer Pole Length on the Optical Properties in Gemini Lens", International Academic Institute for Science and Technology, International Academic Journal of Science and Engineering, Vol.10, No.2, 2023, pp.89-95. ISSN 2454-3896.University of Kirkuk.
14. M. J. Ahmed, and M. A. Hussein, 'Computation Design to Simulate an Objective Magnetic Lens and Study of Effect the Distance Between Pole pieces on its Optical Properties', Journal of Current Researches on Educational Studies, 12 (2), 67-76, 2022.
15. R. Y. J. AL-Salih, and J. A. Aljibory, 'Comparison Between the Properties of Three New Designs of Pinhole Magnetic Lens', Tikrit Journal of Pure Science (2024) 29 (1):119-127, 2023.
16. E. Abdulmajeed, and M. A. Hussein, 'Effect of Changing Distance between Poles on Optical Properties of Gemini Lens' IRAQI JOURNAL OF APPLIED PHYSICS, pp. 411-415, Vol. 20, No. 2B, May 2024. University of Kirkuk.
17. A. Khursheed, 'The Finite Element Method in Charged Particle Optics'. 1999.
18. B. Lencovà, 'Program AMAG for computation of vector potential in rotationally symmetric magnetic electron Lenses by FEM', Inst. Sci. Instrum. Czech. Acad. Sci. Brno, Czechoslovakia, pp.1-58, 1986.

International Journal of Information technology and Computer Engineering
ISSN: 2455-5290
Vol: 04, No. 06, Oct-Nov 2024
http://journal.hmjournals.com/index.php/IJITC
DOI: https://doi.org/10.55529/ijitc.46.1.17

19. E. Munro, 'Munro's electron beam software MEBS', Report, MEBS Ltd., London SW74AN, England, 2011.
20. B. Lencovà, and M. Lenc, 'Paraxial trajectory computation in magnetic electron lenses', Optik, Vol. 82, No. 2, pp. 64-68, 1989.
21. W. M. Murad, 'Design of iron-free magnetic electron lenses', M.Sc. Thesis, The University of Mosul, Iraq, 1998. (in Arabic).
22. B. Lencová, and J. Zlámal, A new program for the design of electron microscopes. Physics Procedia, 1(1), 315-324, 2008.
23. B. Lencová. 'On magnetic lens computations with FEM and BEM', Nuclear Instruments and Methods in Physics Research A 519, pp. 133.